Modelling of Underwater Acoustic Networks for Source Localization in Arbitrary Bounded Reservoirs

Sanjoli Narang, Aditya Harakare, Nayan Barhate, Andrews Varghese, Aayush Shrivastava, Ayushi Gupta
Student Members, AUV-IITB
IIT Bombay,
Mumbai, India
sanjoli.yg@gmail.com, adityaharakare1@gmail.com, nbarhate151@gmail.com, andrewsgeorgevarghese@gmail.com

***Abstract*—In this paper, a non-statistical MATLAB-based software model for a bounded shallow underwater acoustic network comprising an arbitrary number of transmitters, receivers and the water channel is presented. The model is constructed to highlight the non-ideal behavior of the underwater channel including attenuation, reflections, multipath effects, noise and phase-frequency shifts. To highlight the utility of the model, a Time-Difference-Of-Arrival (TDOA) algorithm to locate an underwater sound source using a hydrophone array is tested on the model and the received signals are observed to show realistic results as if they have actually propagated through the water channel. Such a network model can be used to test localization algorithms for any acoustic source, without the need to gather real data in the specific water reservoir.**

***Index Terms*—Underwater channel modelling; TDOA; Localization algorithms ; Multipath**

I. Introduction

The mathematical modelling of underwater shallow acoustic channel has been the prime targets of many previous works [1], [2] on the development of efficient communication and localization systems. The dynamic nature of the marine environment, (including the complex noise functions, multipath effects [3], multiple reflections from the sea bed and attenuation due to absorption) becomes a time-bottleneck to the development of such systems. To eliminate the phase of repeated preliminary testing of the systems directly in the water, an accurate data-processing model becomes important. A data generating model in many cases can save the time of deployment of many acoustic sources, sensors and the time of acquiring the enormous data from the actual water reservoirs. Through this paper, we present a light but sophisticated model of an underwater channel and highlight its characteristics including attenuation, noise, multipath effects and prominent reflections. The model specifically replicates a bounded water body, where the reflections from the bounding walls and the water surface have prominent effects on the acoustic signals thereby causing signal interference at the receivers. This is unlike the unbounded reign of the oceans where reflections occur mainly at the air-water interface. The model can simulate a complete underwater acoustic sensor network with arbitrary sources, sinks and controllable channel behavior aiding to the testing of underwater Global Positioning Systems (GPS) to track the locations of these source nodes under user-adjustable conditions. A time difference of arrival (TDOA) based underwater source localization scheme is also tested on the model data to emphasize on its utility.

II. Methods and results

Given the position co-ordinates of the sources and the receivers, along with the dimensions of the reservoir, a water channel link is established between each combination of the source and the receiver. Such a link consists of many possible paths from the source to the receiver including the Line-Of-Sight (LOS) transmission and the dominant reflections from all possible surfaces. For each path in the link, the signal attenuates with the propagation distance, and underwater noise from different sources gets added to the signal. Other less prominent sources of disturbance includes the thermal noise in transducers and sensors. At the receiver end, the signals propagated through each of these paths in the link get combined from all the sources and a time-series is obtained.

A. Propagation noise

The impact of surface noise is much more prominent in shallow water systems than in oceans but the turbulence noise is lesser. Each of the noise sources including surface turbulence, commuting of aquatic fauna, ships generates noise signals that can possibly be of different bandwidth [2]. The power spectral density (PSD) of the noise, therefore, is expected to be continuous throughout the frequency scale, although in accordance with the Wenz model [4] the noise is colored, its distribution is roughly Gaussian and its power spectral density (PSD), (*N(f)*) is estimated by the empirical formula : $N(f) = N_t(f) + N_s(f) + N_w(f) + N_{th}(f)$, where the N_t, N_s, N_w, N_{th} represent the PSD in dB per Hertz for the turbulent, shipping, wind and thermal noise respectively. These are individually calculated using the formulation given in [4] and added afterwards.

$$N(f) = N_t(f) + N_s(f) + N_w(f) + N_{th}(f) \tag{1}$$

$$\log(N_t(f)) = 1.7 - 3\,\log(f) \tag{2}$$

$$\log(N_s(f)) = 4+2(s-0.5)+2.6\,\log(f)-6\,\log(f+0.03) \quad (3)$$

$$\log(N_w(f)) = 5+0.75w^{0.5}+2\,\log(f)-4\,\log(f+0.4) \quad (4)$$

$$\log(N_{th}(f)) = -1.5+2\,\log(f) \quad (5)$$

where f is the frequency and s, w are the speeds of the ship and the surface winds respectively. The noise power is converted into a time domain signal by constructing a sample frequency spectrum of the noise where the magnitude response is obtained using the power spectral density and the phase is generated using a random number generator. The time domain signal obtained by taking its inverse Fourier Transform should be real, therefore the phase response is adjusted to ensure complex conjugate symmetry in the Fourier Transform. The Signal to Noise ratio is a user-controllable parameter obtained by comparing the power of ambient noise in the reservoir to the power rating of the acoustic source for the given testing conditions.

B. Attenuation and Absorption

The electromagnetic waves incur large attenuation while travelling in water as compared to acoustic waves for high frequencies, due to path fading, spreading loss and absorption, thereby making the acoustic waves preferable for long-distance transmission. The spreading loss for an acoustic wave is obtained using the range of transmission in (6).

$$PL_{spread}(R) = k \times 10\,\log(R)[dB] \quad (6)$$

where R is the range in meters and k is the spreading factor, and PL_{spread} is the incurred spreading loss. When the medium through which the signal is transmitted, is unbounded, the spreading is spherical and the spreading factor is $k = 2$ whereas in bounded spreading, it is considered as cylindrical with $k = 1$. In practice however, an average spreading factor of $k = 1.5$ is often considered [3].

The acoustic waves incur path loss due to absorption of sound by the medium while travelling, and is characterized by the absorption coefficient, α of the surfaces and the medium. [5] The dependence of the parameter α on frequency is complicated, having a piece-wise variation with the actual frequency range, and the exact end points of this range differ in literature. The dependence of α on frequency is however, best modelled by the equation given by Thorp (1967) for frequencies below 50 kHz [3].

$$PL_{absorption}(R) = 10 \times \log(\alpha(f)) \times R[dB] \quad (7)$$

As mentioned in [6] and [7], the net path loss is the additive contribution of both the spreading and absorption losses.

$$PL_{total} = k \times 10\log(R) + 10\log(\alpha(f)) \times R[dB] \quad (8)$$

C. Reflections

In transmitting a signal from an acoustic source to a receiver in a closed reservoir, multipath effects are often observed. The signal gets reflected from the four sidewalls, the reservoir base and the air-water surface undergoing both the phase variations and a surface-dependent attenuation. All the reflected signals interfere at the receiving point with the signal transmitted along the line-of-sight. The reflected signals travel a longer path and hence are a delayed and weakened versions of the direct line-of-sight signal. Given the positions of the sources, receivers, and the nature of reservoir surfaces, the point of reflection is computed geometrically, using the standard laws of reflection, assuming negligible bending of the waves. The reflected waves with attenuated amplitudes, are thus generated with the point of reflection as their starting point and transmitted along their line-of-sight. The reflection coefficients depend on the nature of the surface and are calculated using the Rayleigh formulation [8]. For the water-bottom/side wall interfaces and the air-water surface, the reflection coefficients r_b and r_s respectively are expressed in (9) and (10)

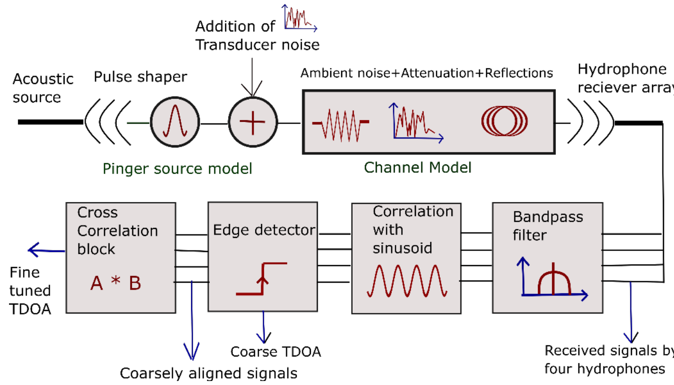

Fig. 1. Block diagram describing the modelling of the acoustic source, various sources of underwater and sensor noise, the channel model in MATLAB and the scheme used for localization of acoustic source by measuring the time difference of arrival (TDOA). There is one block for computing cross-correlation followed by edge detection of output computes the coarse TDOA. The fine-tuning is done by auto-correlation of the four sinusoidal pulses received

$$|r_b| = \frac{m\cos(\theta) - \sqrt{n^2 - \sin^2(\theta)}}{m\cos(\theta) + \sqrt{n^2 - \sin^2(\theta)}} \quad (9)$$

$$|r_s| = \sqrt{\frac{1+(\dfrac{f}{f_1})^2}{1+(\dfrac{f}{f_2})^2}} \quad (10)$$

where $m = \frac{\rho_1}{\rho}$ $n = \frac{c}{c_1}$, $f_2 = 378w^{-2}$ and $f_1 = \sqrt{10}f^2$, ρ and c are the density and sound speed respectively for water, ρ_1 and c_1 are density and sound speed respectively of the base of the reservoir, w is the velocity of wind and f is the operating frequency of the acoustic source.

III. Discussion

In the first part, the actual experiment is performed for ALP-365 acoustic source that generates a sinusoidal pulse of duration two milliseconds (the 'ping' signal) periodically every two seconds in a rectangular reservoir of dimensions

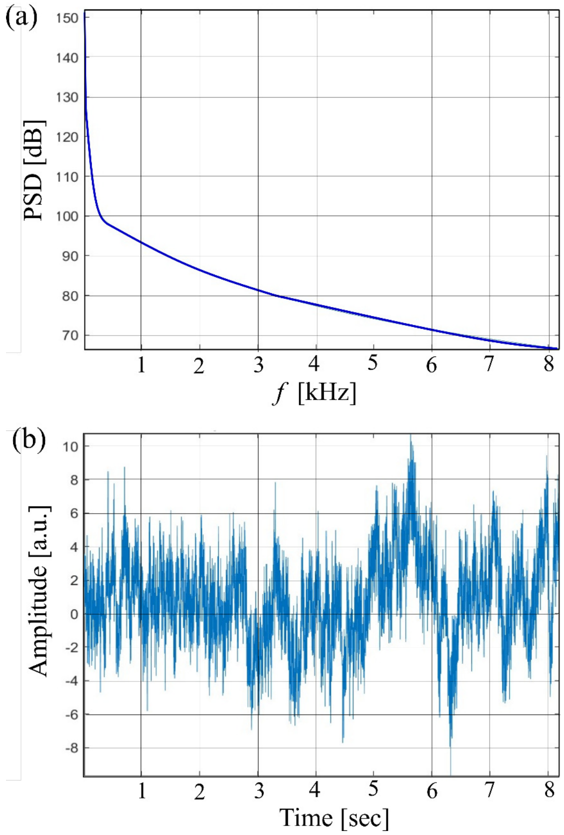

Fig. 2. Illustration of conversion of the noise (a) power spectral density (PSD) to (b) time-series. The sampling rate is 10 kHz and the noise is a combination of white, pink (PSD $\propto \frac{1}{f}$) and red (PSD $\propto \frac{1}{f^2}$) modes. The time-series data generated by random phase method mirrors this behavior by its fast varying components(white) riding on slow varying components(red)

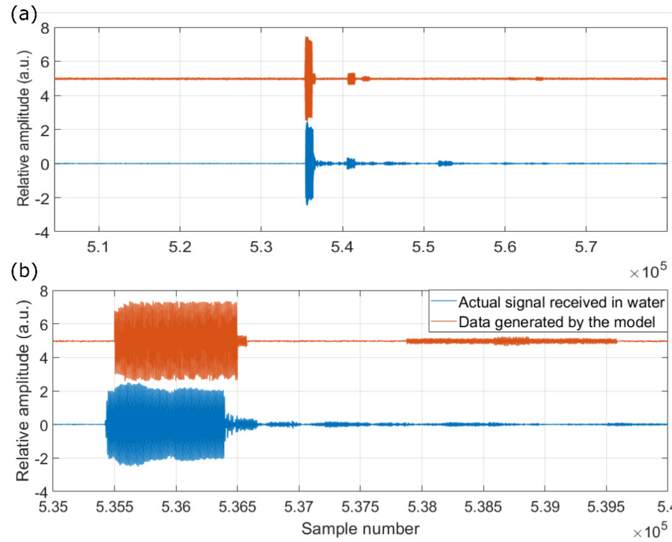

Fig. 3. Output of the proposed Model compared with the actual data sampled from the Teledyne RESON TC4013 Hydrophone placed inside a swimming pool. The acoustic signal shown in the figure is received at the point (45,20,-0.5), while it is sourced from the point (40,11,2.5) with an SNR of 80 at the transducer. The ping signal has a frequency of 45KHz and emits a sinusoidal pulse of duration 2 ms. In the model, the ping signal is shaped using a Tukey window with taper coefficient of 0.002 and receiver and transducer noise are added artificially. The sampling rate of the receivers in both the cases is 500 Ksps. (a) shows a broader time view with many prominent reflected pings aligning in the model as well as the real scenario. (b) shows a zoomed in view of the major ping signals and their similarity

50x25x3. The source can emit acoustic waves of any frequency between 20 kHz and 50 kHz. The data is received by an array of four Teledyne RESON TC4013 hydrophones placed at the four corners of a small square. The acoustic source is placed at (42, 16, -2.5), and the transmitted signal is received by the array consisting of four hydrophones at (45, 20, -0.5), (44.8, 20, -0.5), (45, 19.8, -0.5), (44.8, 19.8, -0.5).

In the second part, a model of the above setup is constructed with sources and receivers placed at same positions inside the rectangular reservoir of same dimensions. The underwater channel model has all the discussed non-ideal channel effects as present in the actual testing area. For modelling the acoustic source, ALP-365, a sinusoidal pulse with a Tukey window is used since the transducer has a finite reaction time to the stimulus and hence the pulse is not perfectly rectangular. A slowly rising/falling function envelopes the pulse with an adjustable taper coefficient. The noise due to the thermal energy of the transducer, is assumed to be zero mean Additive White Gaussian Noise, whose variance is calculated using the equipartition of energy. Similarly, the noise at the receiver points is modeled and added to the signal upon reception. A sample rate of 1 Msps and a precision of 16-bit is used for the processing of the generated data. The modelled source signal is passed through the channel model and the output is used as the received data. The entire flow is described in the figure(1)

A comparison is made between the transmitted acoustic signal in the actual experiment and the signal transformed similarly by the model. Figure(3) compares the raw time series data received at the hydrophone array after transmission with the data generated and altered by the channel model for same positions of transmitters and receivers. One can see similar effects of the multiple reflections in the form of small delayed pulses of same duration and the oceanic noise on the both the signals. Figure(4) shows the same acoustic signal, the sinusoidal ping and the reflections as received by the four hydrophones in the array with different instants of arrival.

A Time Difference Of Arrival (TDOA) based algorithm is tested on the data received by the hydrophones in the model as described by the block diagram in the figure(1) also. The incoming data at the receivers is sampled at 1 Msps for 200 ms. Then a spectrum based analysis is used to detect the presence of a ping in the current bin. If the ping signal is present, further calculations take place. Since the pulse is approximately sinusoidal with an envelope riding on it, the crude starting instants of the signals are computed using sine-correlation followed by edge detection as shown in the figure(5). Cross-correlation is a widely used measure of finding similarity between two signals.For simplicity, the ping signals from two hydrophones say $g(t)$ and $f(t)$, after filtering can be approximated to be just time shifted versions of each other, therefore for the sample rate of $F_s = \frac{1}{T_s}$, if NT_s is the time

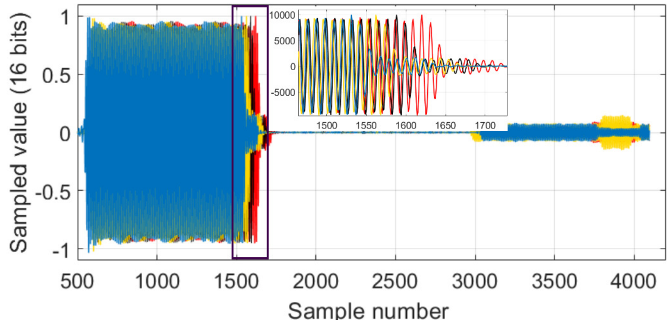

Fig. 4. Normalized sinusoidal pulses received by the four hydrophones of the array, in the simulation model. The signals are time shifted with respect to each other due to difference in the hydrophone positions. Less intense pulses are also captured that arise due to reflections and multipath while propagating from the source through the channel.

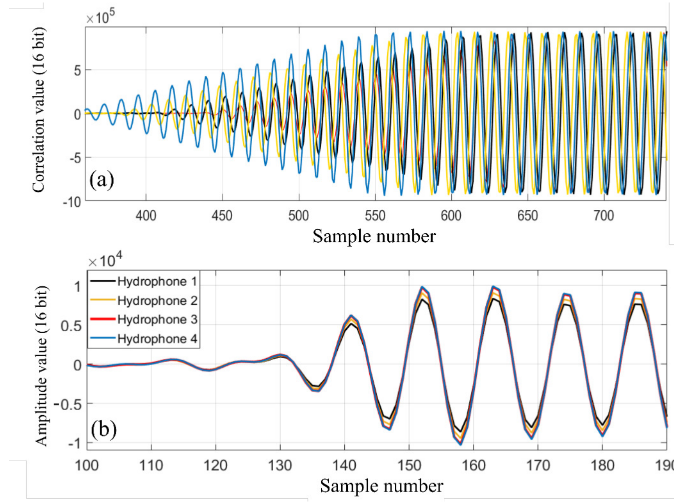

Fig. 6. (a) Cross-Correlation of the received signals to compute the time of their arrivals. (b) The signals aligned according to the fine-tuned time difference computed after cross-correlation

difference between the two signals then $g[n] = f[n - N]$.

$$(f * g)[n] = \sum_{k=-\infty}^{\infty} f[k] \times f[n + k - N] \tag{11}$$

Since a signal can have maximum correlation with itself instead of its shifted versions, for non-periodic signals the correlation function reaches maximum for $n = N$. After correlating with sine, a rough estimate of the starting points is achieved and the four pings are aligned using this estimate. To refine the TDOA values, cross-correlations between the four signals is performed and the peaks of the output are identified. The output of the cross-correlation between each of the four received signals at each receiver and the time-aligned signals are shown in the figure(6). A refined TDOA estimate is achieved which can later be used for position calculation using exact geometrical solutions or the YDSE approximation. The algorithm when applied on the data generated by the model correctly computes the time difference between the signals without any trivial or frivolous results.

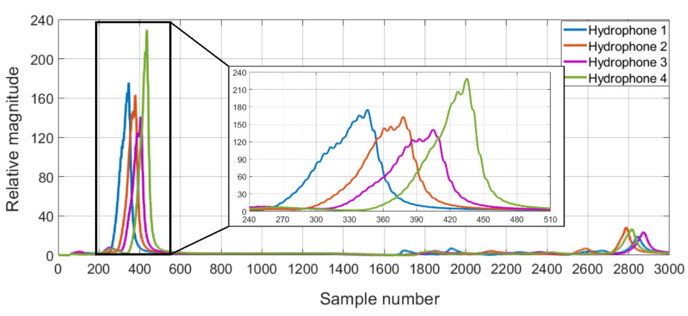

Fig. 5. The output peaks of the edge detector is used to coarsely align the ping signals. The peak denotes the coarse time shift between the received signals. Notice that the smaller peaks pertaining to the reflected waves are also sensed at the end of the time window

IV. Conclusion

A light-weight simulation and modelling platform for underwater acoustic network was proposed in the paper, specifically for the fast development of newer algorithms for localization. The analysis performed on the model data for Time Difference Of Arrival localization scheme, can be very well used for the characterization of any other localization method. The sound source can be placed on a moving vehicle/body underwater and its position and velocity can be tracked by the receiving array in real time. The future sees itself full of novel localization methods based on data-driven algorithms, whose performance depends on the raw data available for use. Future prospects should be circling around on how to modify time asynchronous localization algorithms to include the effects of multiple sources of sound in a reservoir. In such a case, a test-bench like the one proposed in the paper would be critical.

References

[1] S. Ahmed, S. S. Zaidi, R. Khan, and A. Wala, "Underwater acoustic channel modeling using bellhop ray tracing method," 01 2017, pp. 665–670.

[2] X. Wang, X. Wang, R. Jiang, W. Wang, Q. Chen, and X. Wang, "Channel modelling and estimation for shallow underwater acoustic ofdm communication via simulation platform," *Applied Sciences*, vol. 9, no. 3, 2019. [Online]. Available: https://www.mdpi.com/2076-3417/9/3/447

[3] T. Melodia, H. Kulhandjian, L.-C. Kuo, and E. Demirors, *Advances in Underwater Acoustic Networking*. John Wiley Sons, Ltd, 2013, ch. 23, pp. 804–852. [Online]. Available: https://onlinelibrary.wiley.com/doi/abs/10.1002/9781118511305.ch23

[4] P. Qarabaqi and M. Stojanovic, "Statistical characterization and computationally efficient modeling of a class of underwater acoustic communication channels," *Oceanic Engineering, IEEE Journal of*, vol. 38, pp. 701–717, 10 2013.

[5] Z. Babar, Zongxin Sun, Lu Ma, and Gang Qiao, "Shallow water acoustic channel modeling and ofdm simulations," in *OCEANS 2016 MTS/IEEE Monterey*, 2016, pp. 1–6.

[6] F. De Rango, F. Veltri, and P. Fazio, "A multipath fading channel model for underwater shallow acoustic communications," in *2012 IEEE International Conference on Communications (ICC)*, 2012, pp. 3811–3815.

[7] G. Burrowes and J. Y. Khan, "Short-range underwater acoustic communication networks," in *Autonomous Underwater Vehicles*, N. A. Cruz, Ed. Rijeka: IntechOpen, 2011, ch. 8. [Online]. Available: https://doi.org/10.5772/24098

[8] L. Emokpae and M. Younis, "Surface based underwater communications," 01 2011, pp. 1 – 6.